

Detection of Spread-F, foF2 values and Planetary and Gravity Wave Signatures using Digisonde instruments and their comparison with COSMIC-I/FORMOSAT-3, SAMI and IRI data

Preeti Bhaneja

ABSTRACT

Statistical studies of spread F for midlatitude and low latitude regions using digisonde data. Various algorithms have been written to process the raw data and determine spread F by using edge detection and pattern recognition techniques. Algorithms have also been written to find foF2 and hmF2 values for obtaining the density profile of the ionosphere. Findings based on work carried out to date include:

- Determination of seasonal and solar cycle variation patterns.
- Correlation between digisonde, COSMIC-1/FORMOSAT-3 satellite data and SAMI and IRI models values to check for validity of data.
- Wave analysis has been performed to detect the presence of planetary and gravity wave patterns in foF2 values with periods ranging from a few hours to a few days and also for various seasons.

INTRODUCTION

Density irregularities in the ionosphere are often observed as a spread pattern in data from radio sounding techniques such as digisondes referred to as Spread F. Spread F is observed at both mid latitudes called Midlatitude Spread F (MSF) and equatorial latitudes called Equatorial Spread F (ESF); both are caused by different instability mechanisms due to the angle of the magnetic field relative to the ionospheric plasma layer.

Ionospheric F region is known to exhibit anomalies and irregularities during both day and night time. Various anomalies have been observed in the ionospheric F2 region as observed in the critical frequency and the electron density values. Ionospheric irregularities are temporal and spatial variations of the electron density lasting from a few minutes to several hours.

Planetary wave signatures (PWS) observed in the ionosphere occur either due to the planetary waves (PW) in the mesosphere-thermosphere (MLT) region or due to geomagnetic activity variations with observed wave periods of 2-3, 5-6, 10, 16, 23 and 35 days [Aladill & Apostolov, 2003]. These waves propagate towards the ionosphere creating wave oscillations as observed in the density observations. Atmospheric buoyancy waves, commonly referred to as gravity waves are generated from a variety of sources, including thunderstorms [Lay et al., 2015; Rishbeth, 2006] and auroral disturbances [Nygren et al., 2015; Wickwar & Carlson, 1999].

Gravity waves are considered to be a seeding mechanism that creates density perturbations in the ionosphere leading to spread [Rishbeth, 2006; Lastovicka, 2006;]. Spread-F is a night time phenomenon where the irregularities are observed on the ionograms which are plots of frequency vs. height obtained by reflections of the transmitted signal into the ionosphere when they match the plasma frequency [Bhaneja et al., 2009, 2018]. For equatorial spread F, the various irregularities or spread patterns may be associated with multiple types of plasma structures, such as plumes, patches, bubbles, and blobs [Aarons, 2001].

The data in O-Mode trace is used to generate ionograms for identifying spread F. Ionograms obtained during spread F events show thickness or spread in the F region trace that is significantly greater than that obtained for a normal ionosphere. Figure 1 shows four ionograms indicating different conditions of the ionosphere. 1(a) indicates a quiet ionosphere, represented by a single trace. 1(b), (c) and (d) show ionograms with thick traces which implies strong spread conditions. The spread observed on the ionograms can be classified as range or frequency spread. **Range spread** refers to a condition in which there are multiple range echoes at each frequency. **Frequency spread** refers to the case in which multiple frequencies appear for each altitude. Figures 1 (b), (c), (d) show range, range and frequency spread F and spread F in the form of a big blob respectively.

The boxes shown are positioned by our autonomous edge detection software. Large pixel counts in box 1 correspond to range spreading (RS), and large pixel counts in box 2 correspond to frequency spreading (FS).

ACKNOWLEDGMENTS

The data for all the plots have been provided by NGDC, SPIDR, SPDF, COSMIC, IRI and SAMI.

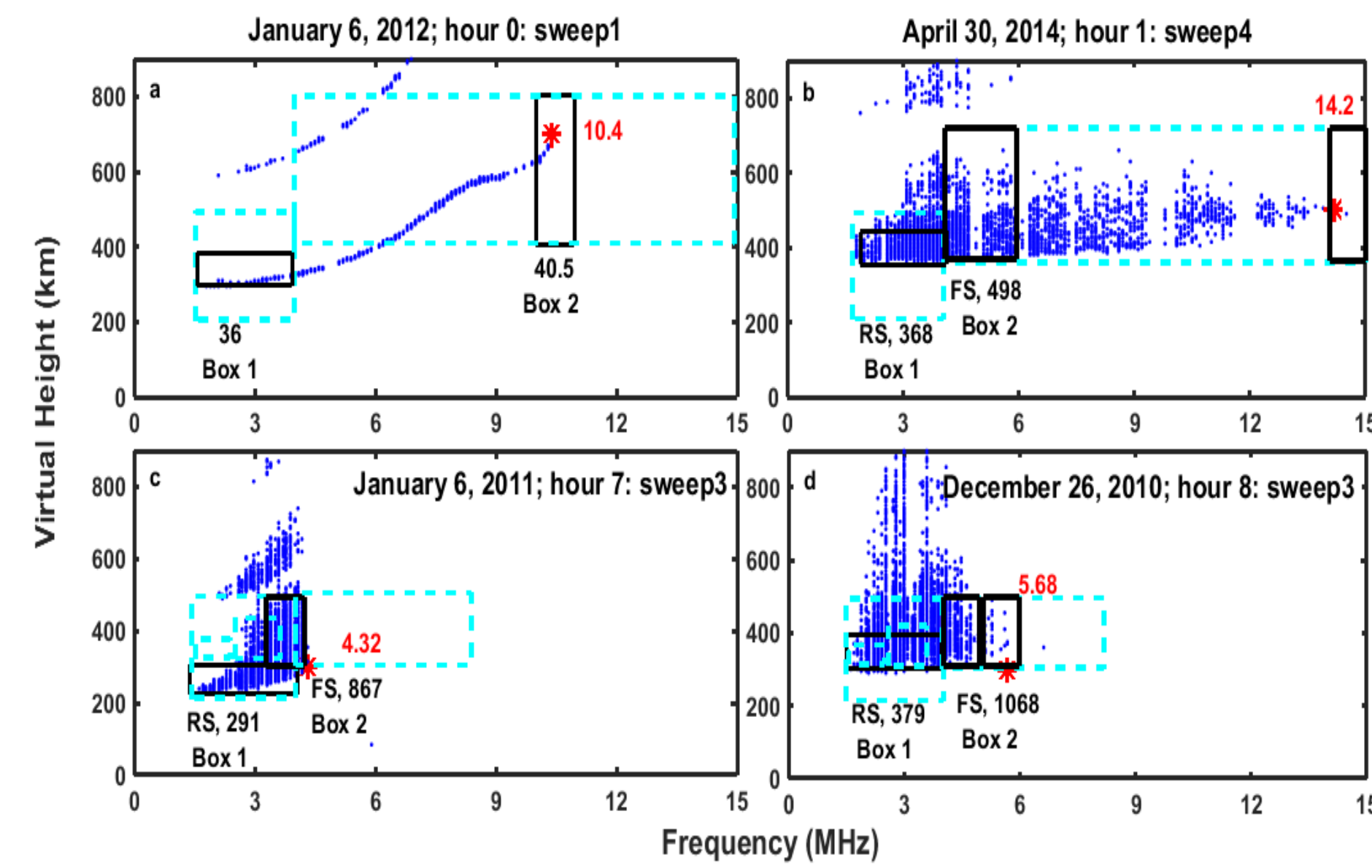


FIGURE 1 – a) An ionogram showing a quiet event. Different kinds of Spread F event; b) Range Spread; c) Range and Frequency Spread; d) Spread in a form of a big blob. The left axis is the virtual height in km and the bottom axis is the frequency in MHz. The dotted lines are the boundary boxes and the solid line boxes are selected by the algorithm for determining foF2, RS and FS.

DATA PRESENTATION

Our dataset is comprised of nighttime ionograms at 15 minute intervals. The focus of this study is to determine statistics of spread F events and detect foF2 values and compare them with COSMIC measured, IRI and SAMI models generated values. Figures 2-8 illustrate these findings.

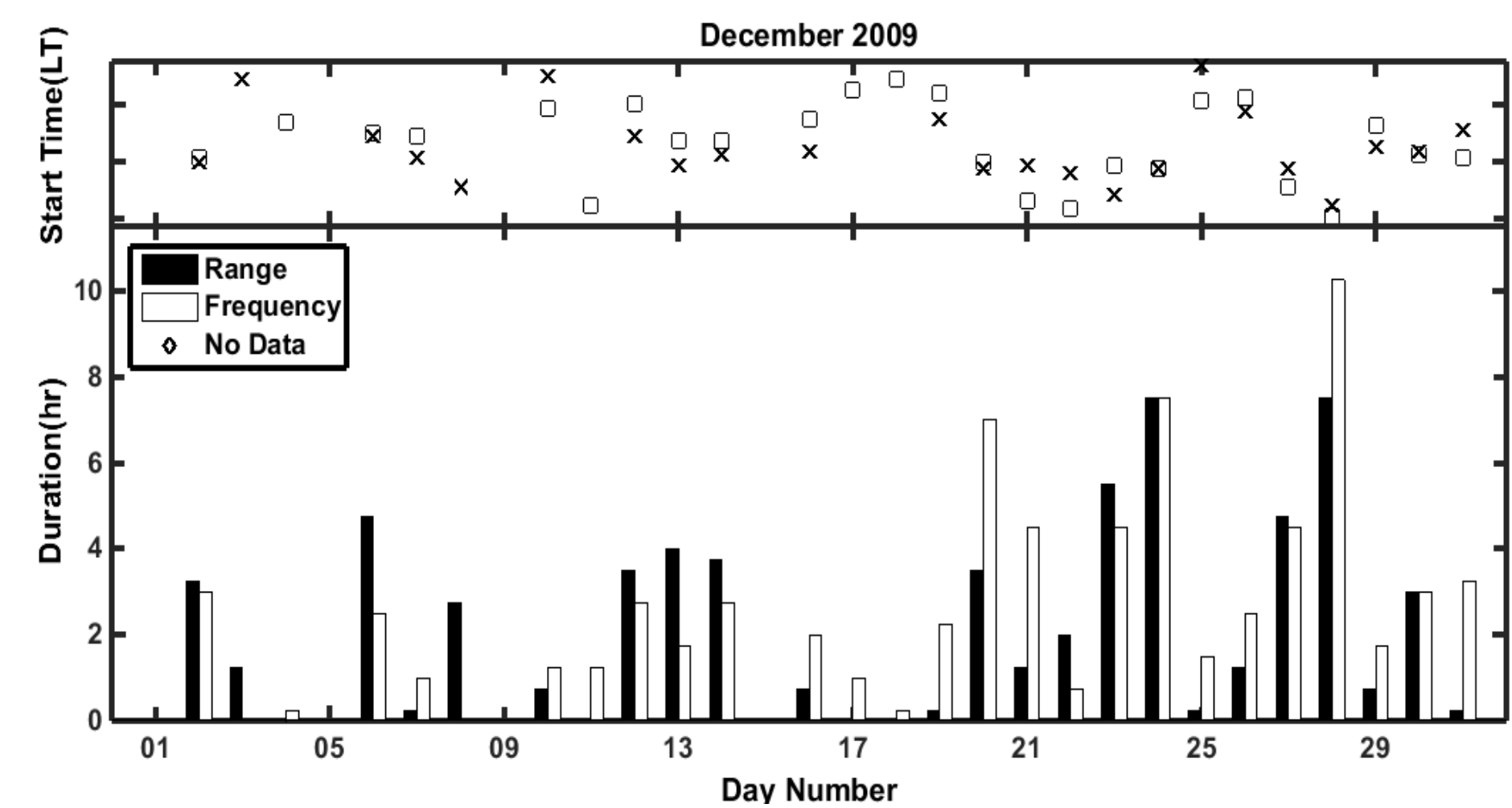


FIGURE 2 –Monthly occurrence plot for December 2009 showing range and frequency spread F onset time and duration for night time hours between 8PM-6AM LT. The cross symbol denotes the start time for range spread F and the square symbol denotes the start time for frequency spread F.

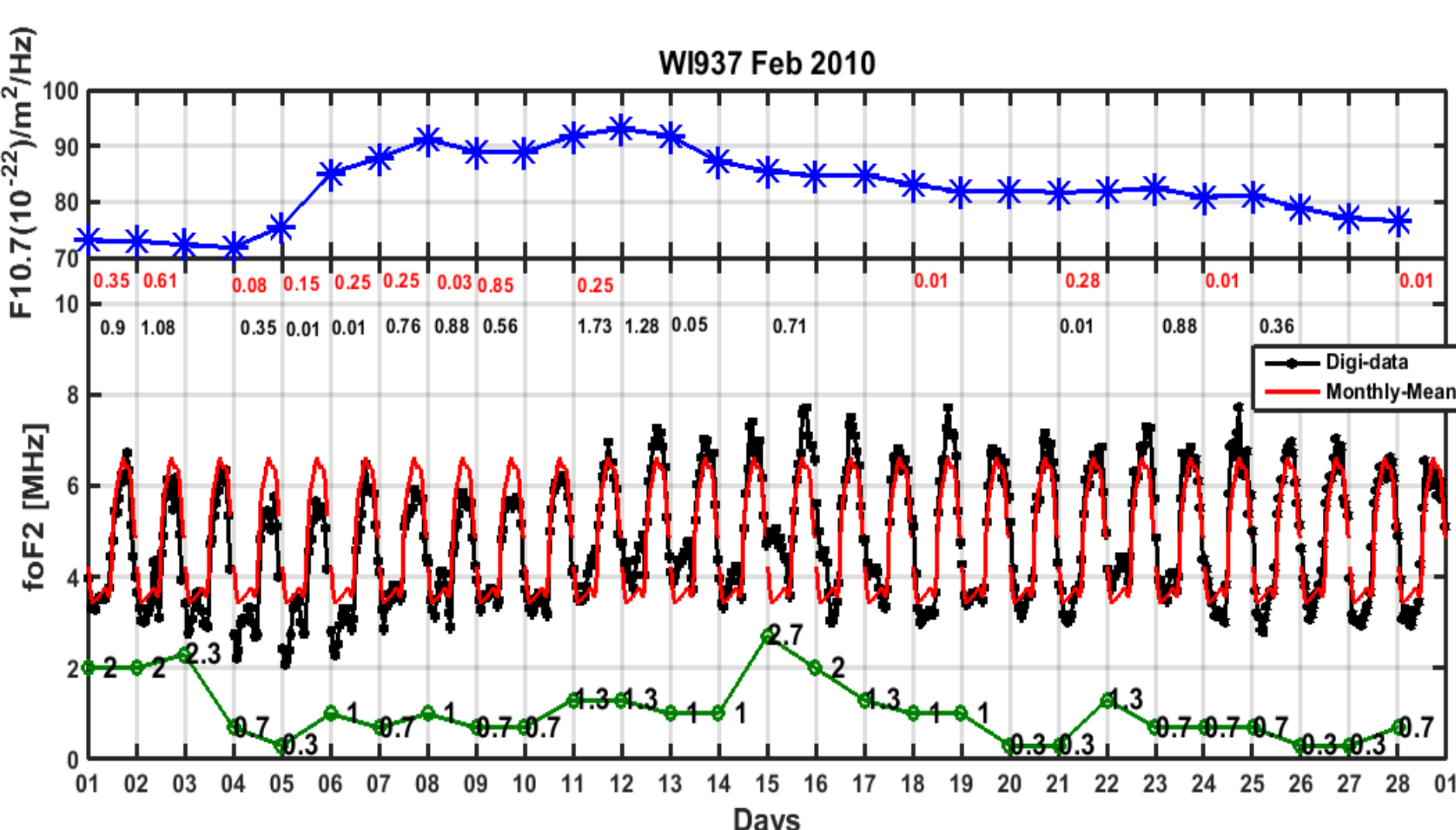


FIGURE 3 –VPIR (Wallops Island) for February 2010. The numbers in red correspond the hours of Range Spread F while the black correspond to Frequency Spread F. The top panel shows the F10.7 values and the green curve represents the kp values.

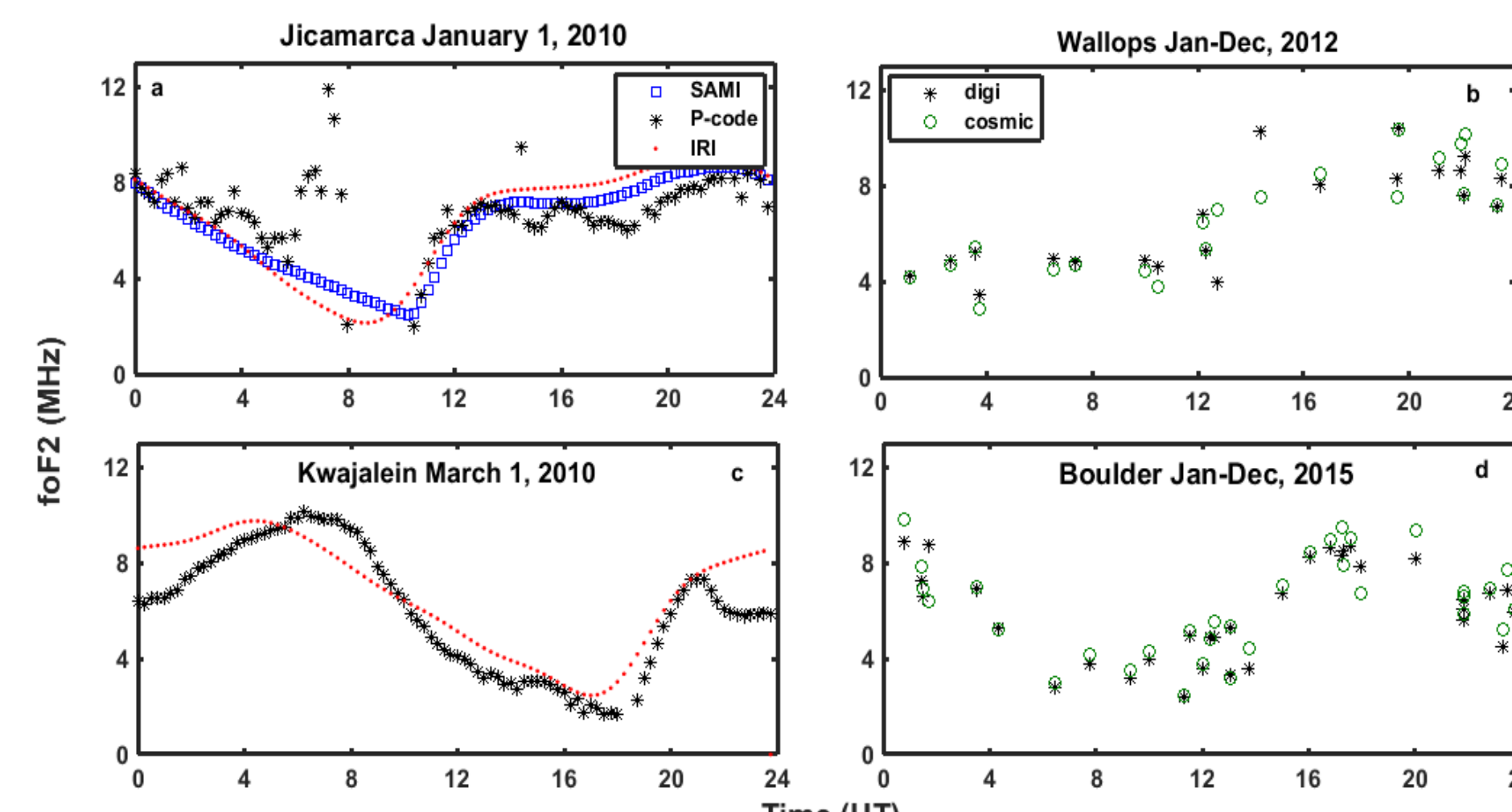


FIGURE 4 – Comparison of foF2 for digisonde data from Jicarcarca, Wallops, Kwajalein & Boulder with COSMIC-1, SAMI and IRI values.

Figures 5 & 6 provide the amplitude spectra of the foF2 values using the Lomb-Scargle periodogram analysis. Figure 5 shows the planetary and gravity wave oscillations in the foF2 values detected from the ionograms. The foF2 values show planetary wave signatures of 2,3,4,7 and 10 days wave oscillations and also presence of diurnal (24 hours), semi-diurnal tides (12 hours) and teri-diurnal tides (8 hours) and gravity wave signatures from 2 to 6 hours. Figure 6 shows the planetary wave period variation for the different seasons of spring, summer, fall & winter.

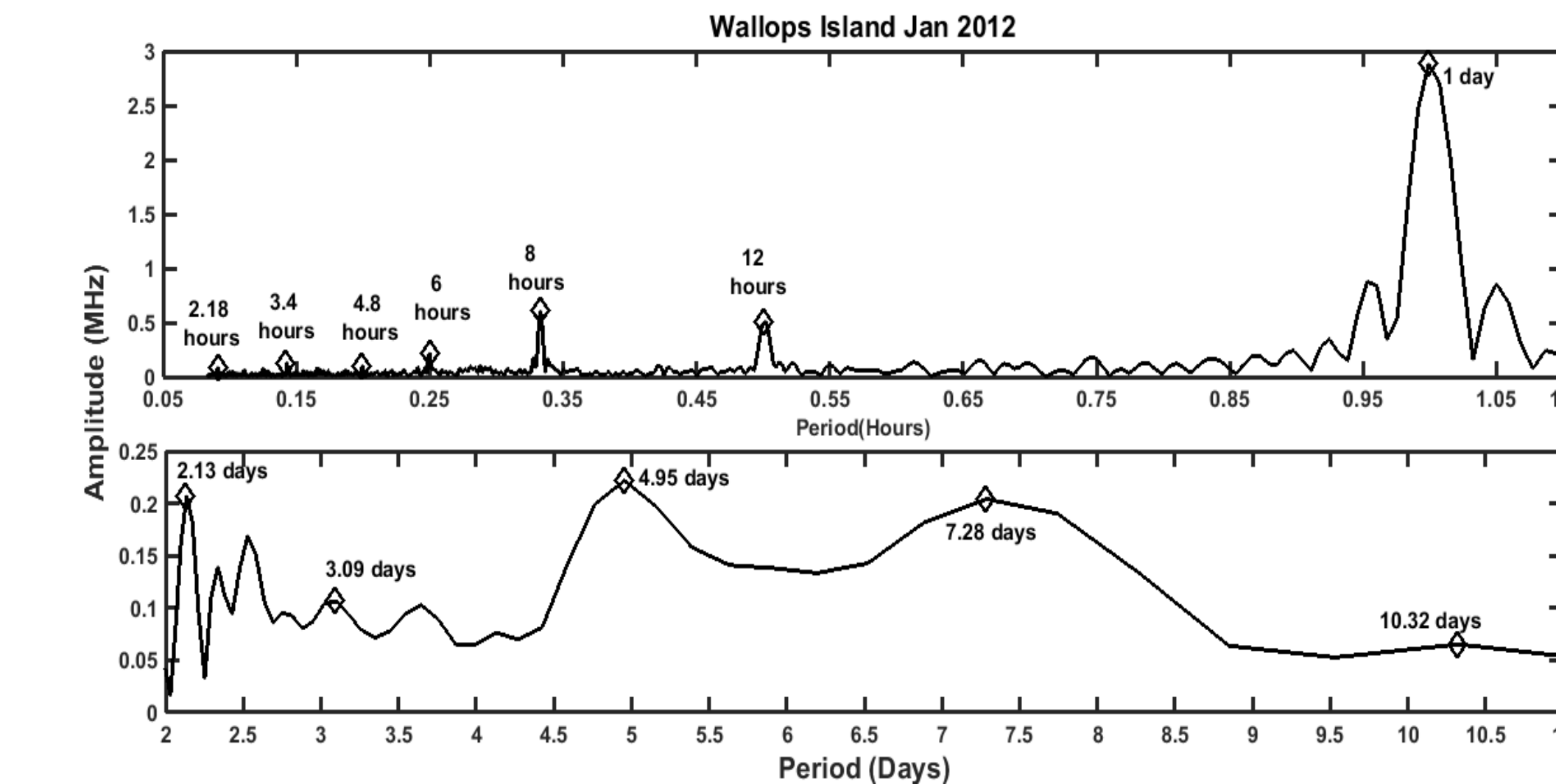


FIGURE 5 – Wave Analysis for foF2 values for Jan 2012. Amplitude spectra of digisonde data (Wallops) for Jan 2012 showing the peak periodicities in the foF2 data.

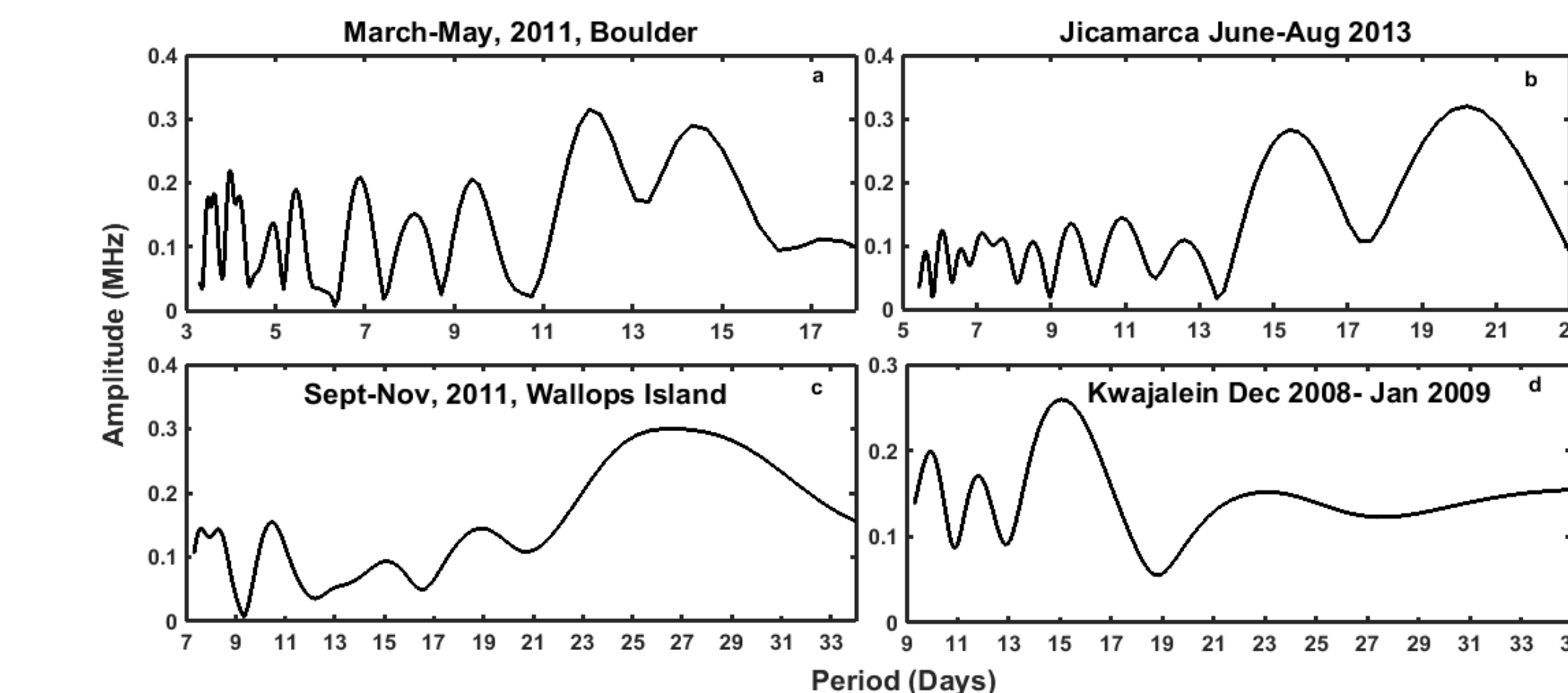


FIGURE 6- Wave periods and Amplitudes for foF2 from Boulder, Jicarcarca, Wallops Island and Kwajalein stations obtained using Lomb-Scargle periodogram analysis for all the four seasons starting from (a) spring season, March – May 2011, (b) summer season, June- Aug 2013, (c) fall season, Sept-Nov 2011 and (d) the winter season, Dec 2008 –Jan 2009.

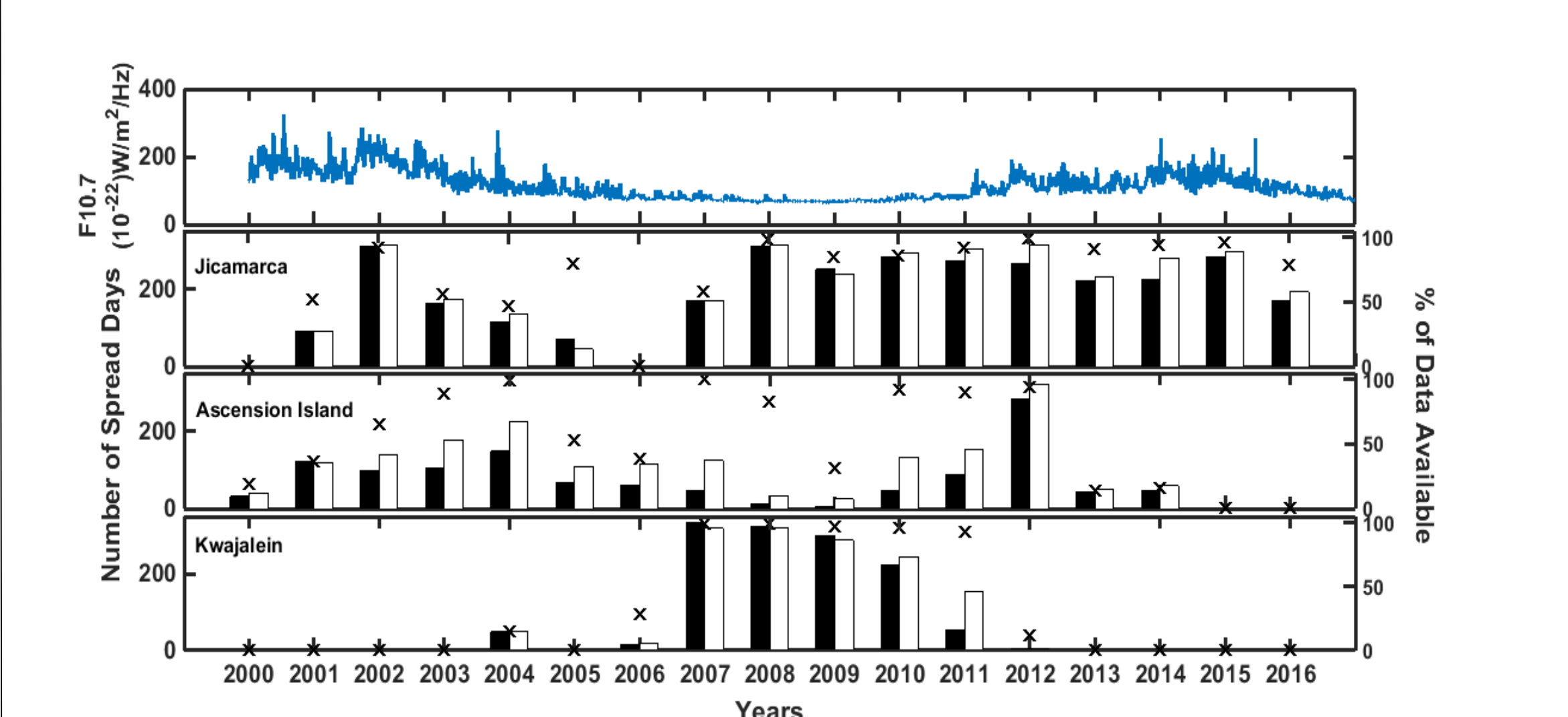
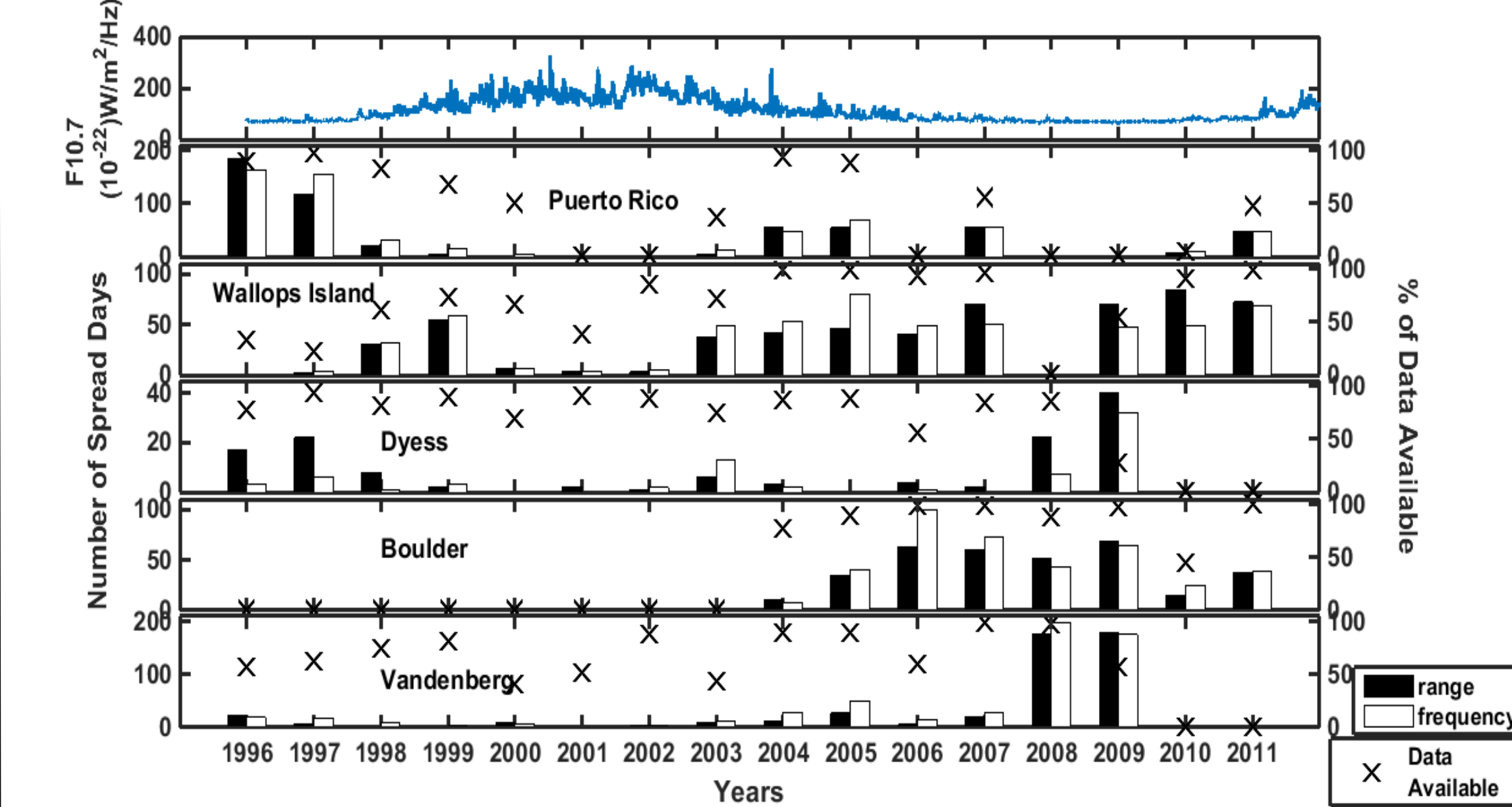


FIGURE 7 –Plots show the solar cycle variation of spread F for midlatitude sites; 16 years (1996-2011) of data for Wallops Island and Puerto Rico; 14 years (1996-2009) for Dyess and Vandenberg and 7 years (2004-2011) of data for Boulder; low latitude sites; 16 years (2001-2016) for Jicarcarca, 15 years (2000-2014) for Ascension Island, and 9 years (2004-2012) for Kwajalein. The top panel shows the solar flux data which is higher during the solar maximum years (2000-2003 and 2012-2015).

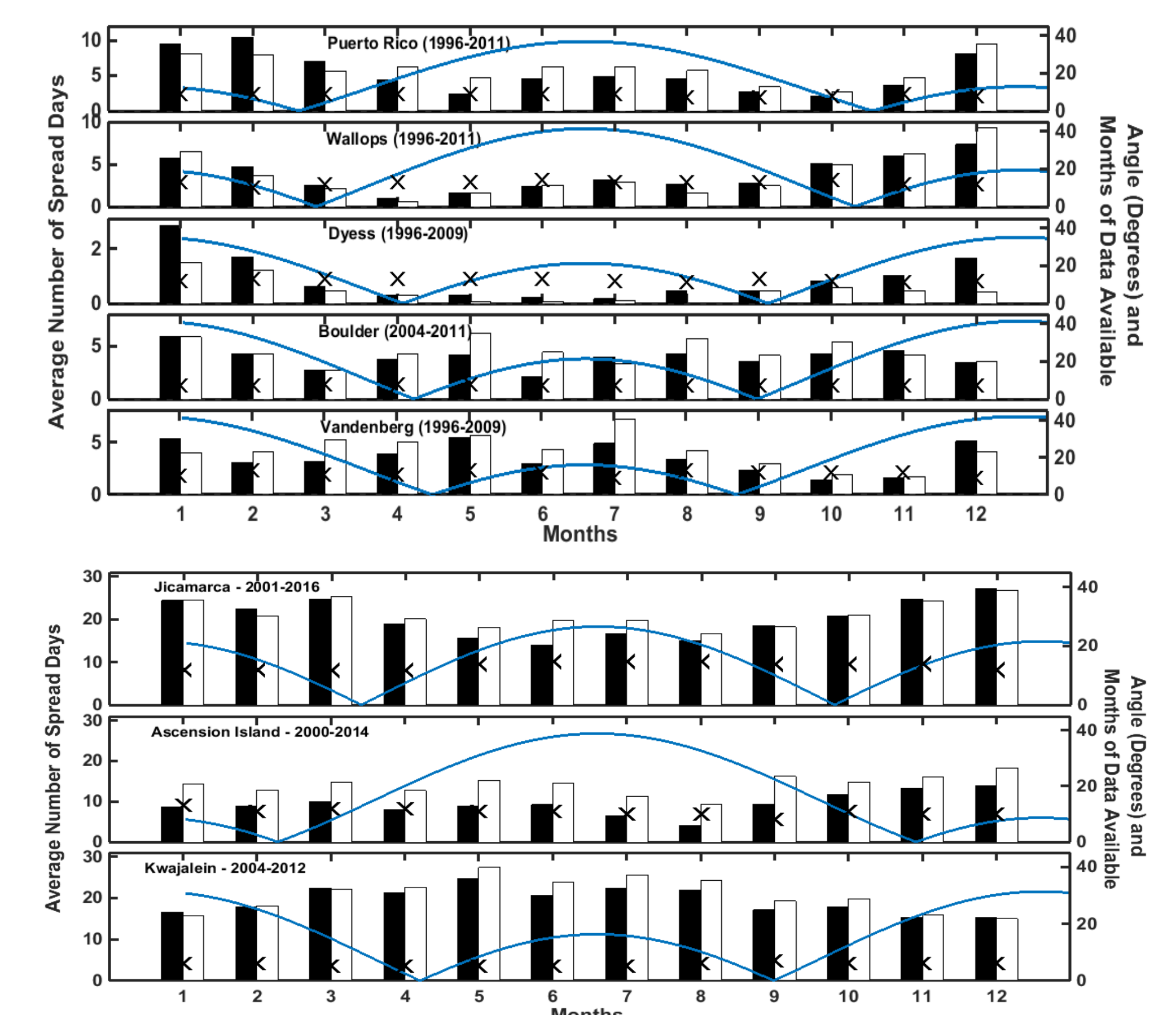


FIGURE 8 – Plot shows the seasonal cycle variation for the sites for the available data. The left-hand side shows the average number of spread days. The right-hand side shows the angle the declination and the terminator and the months of data available. The black bars represent range spread F while white bars represent frequency spread F and the blue line represents the angle.

DISCUSSION

Figures 2 and 3 show a monthly plot of MSF events and foF2 values respectively. It is evident from Figure 4 that the algorithm detects fairly accurate values of foF2 as shown for different stations with data validated by COSMIC satellite measured values and IRI and SAMI model values. Figure 5 shows that the foF2 values have signatures of gravity waves from 2 to 6 hours, teri-diurnal tides (8 hours), semi-diurnal tides (12 hours), diurnal (24 hours) and planetary wave signatures from 2-7 and 10 days wave oscillations. These oscillations may be due to geomagnetic effects or terrestrial weather effects. Figure 6 shows the variation of wave periods with different seasons. The spring season has wave periods starting at 4 days; summer season has wave periods starting from 5 days; fall season show waves from 8 days; winter season shows waves from 10 days and up to 35 days for all these seasons.

Figure 7 shows the solar cycle variation. MSF occurrence rate and duration is higher during solar min than during solar max for all five stations. Equatorial Spread F doesn't have any particular solar cycle variation for the three sites. An interesting observation evident is that almost all stations experience more range spread F events during solar min, and more frequency spread F events during solar max.

Figure 8 shows seasonal variation. All the stations show different seasonal variations, presumably due to their varying longitudes, declinations, or localized forcing from lower altitude sources. The observations are summarized in Table. An interesting observation is that places located at negative declination tend to have most spread F conditions during fall and winter seasons while places at positive declination have most spread F during spring and summer seasons.

Stations	Lat.	Long.	Decl.	Season with max MSF occurrences	Season with min MSF occurrences
Puerto Rico	18.5°	67.1°	-14°	Winter solstice	Spring & Vernal eq
Wallops Is	37.95°	74.5°	-11°	Vernal equinox, winter solstice	Spring equinox, Summer
Dyess	32.4°	99.8°	6.9°	Winter solstice	Spring, Summer, Vernal Equinox
Boulder,	40°	105.3°	10°	Early summer, autumn equinox	Spring Equinox, Winter
Vandenberg	34.8°	120.5°	13°	Summer & winter solstice	Fall
Jicarcarca,	12°S	76.8°	-2.5°	Fall and winter	Spring and Summer
Ascension Is	7.9° S	14.4°	-15.09°	Fall and December	Summer
Kwajalein	8.71°	167.7°E	7.5°	Spring and summer	Fall and winter

FUTURE WORK

- Determine whether MSF is due to MLT region (thunderstorms and lightning) or geomagnetic activity are the predominant cause of MSF.
- Extend the statistical study to high latitude regions.